ISSN 0006-2979, Biochemistry (Moscow), 2011, Vol. 76, No. 2, pp. 186-195. © Pleiades Publishing, Ltd., 2011.
Published in Russian in Biokhimiya, 2011, Vol. 76, No. 2, pp. 226-237.
Originally published in Biochemistry (Moscow) On-Line Papers in Press, as Manuscript BM10-246, January 16, 2011.

# Cys377 Residue in NqrF Subunit Confers $Ag^+$ Sensitivity of $Na^+$-Translocating NADH:quinone Oxidoreductase from *Vibrio harveyi*

**M. S. Fadeeva[1], Y. V. Bertsova[1], L. Euro[2], and A. V. Bogachev[1]***

[1]*Department of Molecular Energetics of Microorganisms, Belozersky Institute of Physico-Chemical Biology, Lomonosov Moscow State University, 119992 Moscow, Russia; fax: (495) 939-0338; E-mail: bogachev@genebee.msu.su*
[2]*Research Program of Molecular Neurology, Biomedicum-Helsinki, University of Helsinki, Haartmaninkatu 8, 00290 Helsinki, Finland; E-mail: Liliya.Euro@helsinki.fi*

Received August 16, 2010
Revision received October 8, 2010

**Abstract**—The $Na^+$-translocating NADH:quinone oxidoreductase ($Na^+$-NQR) is a component of the respiratory chain of various bacteria that generates a redox-driven transmembrane electrochemical $Na^+$ potential. The $Na^+$-NQR activity is known to be specifically inhibited by low concentrations of silver ions. Replacement of the conserved Cys377 residue with alanine in the NqrF subunit of $Na^+$-NQR from *Vibrio harveyi* resulted in resistance of the enzyme to $Ag^+$ and to other heavy metal ions. Analysis of the catalytic activity also showed that the rate of electron input into the mutant $Na^+$-NQR decreased by about 14-fold in comparison to the wild type enzyme, whereas all other properties of $_{NqrF}$C377A $Na^+$-NQR including its stability remained unaffected.

**DOI**: 10.1134/S0006297911020040

*Key words*: $Na^+$-translocating NADH:quinone oxidoreductase, NqrF, ferredoxin:$NADP^+$ oxidoreductase, sensitivity to heavy metals, protein stability

The $Na^+$-translocating NADH:quinone oxidoreductase ($Na^+$-NQR) is a redox-driven sodium pump that generates a transmembrane electrochemical $Na^+$ potential [1]. This enzyme has been shown to operate in the respiratory chain of various bacteria including several pathogenic microorganisms [2, 3]. The enzyme consists of six subunits (NqrA-F) [4] encoded by the six genes of the *nqr* operon [5, 6]. The NqrF subunit is homologous to numerous flavin-containing oxidoreductases.

The C-terminal domain of NqrF resembles ferredoxin:$NADP^+$ oxidoreductases of the FNR family and comprises binding motifs for NADH and FAD [5, 7]. The N-terminal domain shares homology with ferredoxins bearing a [2Fe-2S] cluster and contains four conserved cysteine residues involved in formation of the iron–sulfur center [5, 8]. Thus, NqrF is a polypeptide that combines NADH:ferredoxin oxidoreductase and ferredoxin [7]. The five other subunits of $Na^+$-NQR (NqrA-E) do not have any noticeable homology to other proteins with known functions.

$Na^+$-NQR is thought to contain the following set of prosthetic groups: one [2Fe-2S] cluster, one noncovalently bound FAD, two covalently bound FMN residues, and one noncovalently bound riboflavin [9]. Subunit NqrF binds NADH, FAD, and the [2Fe-2S] cluster [5, 7, 8]. Covalently bound FMN residues are attached by phosphoester bonds to threonine residues in subunits NqrB and NqrC [10], whereas the location of riboflavin in the structure of the enzyme remains unknown [9].

The overall reaction of NADH oxidation and quinone reduction catalyzed by $Na^+$-NQR *in vivo* can be described by the following equation:

$$NADH + H^+_{in} + Q + 2Na^+_{in} \rightarrow NAD^+ + QH_2 + 2Na^+_{out}. \quad (1)$$

This redox reaction is coupled with a vectorial transfer of two sodium ions across the membrane, i.e. the ratio $Na^+/\bar{e}$ for $Na^+$-NQR is 1 [11]. The dependence of quinone

*Abbreviations*: DDM, *n*-dodecyl-β-D-maltoside; dNADH, reduced nicotinamide hypoxanthine dinucleotide; FNR, ferredoxin:$NADP^+$ oxidoreductase; HQNO, 2-*n*-heptyl-4-hydroxyquinoline N-oxide; $K_3$, menadione; $Na^+$-NQR, $Na^+$-translocating NADH:quinone oxidoreductase; NEM, N-ethylmaleimide; Q, ubiquinone; $QH_2$, ubiquinol; $T_m$, unfolding temperature.

* To whom correspondence should be addressed.

reductase activity of $Na^+$-NQR (Eq. (1)) on concentration of sodium ions is hyperbolic, and the value of the apparent $K_m^{Na}$ for the enzyme from *Vibrio* species is about 2-3 mM [12]. $Na^+$-NQR is rather specific to NADH. It does not oxidize NADPH, and among artificial analogs it interacts only with dNADH and thio-NADH [12, 13].

In addition to the native quinone reductase reaction (Eq. (1)), the enzyme can also catalyze a so-called NADH-dehydrogenase reaction [14] that includes a single-electron reduction of soluble quinones ($K_3$, $Q_0$, $Q_1$, etc.) or some other electron acceptors (hexaammineruthenium(III), ferricyanide, etc.). This artificial activity does not depend on the concentration of sodium ions and is not coupled with energy conservation. Only the FAD-binding domain of the NqrF subunit seems to be required for this activity [7, 8].

Only a few inhibitors of $Na^+$-NQR are known. The antibiotic korormicin specifically inhibits $Na^+$-NQR at the level of its interaction with ubiquinone. Korormicin affects the enzyme without competition with quinone, and its inhibition constant is ~0.1 nM [15]. The effect of HQNO on $Na^+$-NQR is similar [16], but the affinity of this inhibitor to the enzyme is significantly weaker (0.3-0.4 μM) [12, 16].

$Na^+$-NQR from *Vibrio* sp. is also sensitive to low concentrations of silver ions [17], to some other heavy metal ions ($Cd^{2+}$, $Pb^{2+}$, $Zn^{2+}$, and $Cu^{2+}$) [13], as well as to SH-reagents [12]. These inhibitors influence the initial steps of the $Na^+$-NQR catalytic cycle and probably prevent interaction of the enzyme with NADH [13].

$Na^+$-NQRs from different bacterial sources have different sensitivity to inhibitors. For example, $Na^+$-NQR from *Azotobacter vinelandii* is not sensitive to low HQNO concentrations [12], $Na^+$-NQR from *Klebsiella pneumoniae* is fully resistant to both $Ag^+$ and N-ethylmaleimide (NEM) [12], while korormicin, a strong inhibitor of $Na^+$-NQR from *V. alginolyticus*, has no effect on the homologous enzyme from *Haemophilus influenzae* [18]. As there was a correlation between inhibition of different $Na^+$-NQRs by $Ag^+$ and NEM, it was proposed that inactivation of $Na^+$-NQR by heavy metal ions is caused by modification of some of its cysteine residue(s) [12]. It was demonstrated previously that isolated NqrF subunit [19] and even the NADH- and FAD-binding domain of the NqrF subunit [7] are still able to perform NADH dehydrogenase activity, and this activity is inhibited by silver ions [7, 19]. These data mean that the $Ag^+$-sensitive cysteine residue must be located in the NADH- and FAD-binding domain of the NqrF subunit. In the present work on the enzyme from *V. harveyi*, it is demonstrated that this reactive residue is $Cys_{NqrF}$-377.

## MATERIALS AND METHODS

**Bacterial strains and growth conditions.** The bacterial strains used in this study are listed in Table 1. *Escherichia coli* cells were routinely grown at 37°C in LB medium. The *Vibrio* strains were grown at 32°C in FM medium as described in [20]. Antibiotic concentrations for *E. coli* were kanamycin at 50 μg/ml, ampicillin at 125 μg/ml, and tetracycline at 10 μg/ml; for *V. harveyi*: rifampicin at 100 μg/ml, kanamycin at 50 μg/ml, and tetracycline at 5 μg/ml; for *V. cholerae*: ampicillin at 150 μg/ml and streptomycin at 50 μg/ml.

**Construction of expression vector bearing the gene encoding a truncated NqrF subunit.** The gene sequence encoding the truncated NqrF subunit (NqrF′, the soluble variant of NqrF containing its Fe-S domain and FAD-binding domain [7]) was amplified by PCR with NQRF′_dir and pBAD_rev primers using pBAD*nqr*4 plasmid [21] as the template. The amplified 1173 bp fragment was cloned into TA-cloning pGEM-T vector (Promega, USA), resulting in the pG7_F′ plasmid. Then the *nqr*F′ fragment was subcloned into pBAD/*Myc*-His (Invitrogen, USA) vector using *Nco*I and *Eco*RI restriction sites, resulting in the pBAD_NqrF′11 plasmid. This plasmid was transferred into *V. cholerae* O395N1 *tox*T::*lac*Z cells by electroporation.

**Site-directed mutagenesis.** Mutagenic primers for substitution of Cys377 to Ala were designed (for the forward primer sequence see Table 1, NQRFC377A_dir). An additional *Apa*I restriction site was built into the primers to facilitate identification of the mutated plasmids by restriction enzyme digestion. Mutagenesis was carried out using the QuikChange II kit (Stratagene, USA) and pBAD_NqrF′11 plasmid as the template. The generated mutant plasmids were checked by *Apa*I restriction, and a correct plasmid (pBAD_C377A) was selected. Then the *Afl*II-*Bpu*14I (781 bp) part of suicide vector pKnFhisAKm [22] was replaced by the *Afl*II-*Bpu*14I fragment of pBAD_C377A (a fragment containing the C377A mutation), resulting in pKn_CA789. This plasmid was used for replacement of the native chromosomal *nqr*F gene of *V. harveyi* with the six-histidine tagged *nqr*F bearing the C377A mutation. To do this, the pKn_CA789 plasmid was transferred into the *V. harveyi* R3 strain via conjugation using *E. coli* SM10λpir as the donor, and a $Tc^S$ $Km^R$ $Rf^R$ phenotype clone (FCA9) characteristic of a double-crossover introduced mutation was selected. The C377A mutation in a *V. harveyi* FCA9 chromosome was confirmed by restriction analysis of an appropriate PCR product.

To express the mutated (C377A) *nqr*F′, the pBAD_C377A plasmid was transferred into *V. cholerae* O395N1 *tox*T::*lac*Z cells by electroporation.

**Membrane vesicles** were isolated from *V. harveyi* cells as described in [23].

**Recombinant His-tagged NqrF′** was isolated from *V. cholerae* O395N1/pBAD_NqrF′11 cells. For *nqr*F′ induction the cells were grown to the middle of exponential phase ($A_{600}$ = 0.3-0.4). After this the growth medium was supplemented with 0.05% of L-arabinose, and the

**Table 1.** Bacterial strains, plasmids, and primers used in this study

| Strains | Genotype or description | Source |
|---|---|---|
| *V. harveyi* R3 | wild type; $Rf^R$ | [20] |
| *V. harveyi* VHtag60 | R3; C-terminal $(His)_6$-tag fusion in *nqr*F; $Km^R$ $Rf^R$ | [22] |
| *V. harveyi* FCA9 | VHtag60; C377A substitution in NqrF; $Km^R$ $Rf^R$ | this work |
| *V. cholerae* O395N1 *toxT*::*lacZ* | nonpathogenic strain of *V. cholerae*; $Sm^R$ | [39] |
| *E. coli* Sm10λpir | *thi thr leu ton*A *lac*Y *sup*E *rec*A::*RP4-2-Tc*::Mu; $Km^R$ | [40] |
| **Plasmids** | | |
| pBAD/*Myc*-His | recombinant protein expression vector; $Ap^R$ | Invitrogen |
| pBADnqr4 | pBAD/*Myc*-His bearing *nqr* operon of *V. harveyi*; $Ap^R$ | [21] |
| pBAD_NqrF'11 | pBAD/*Myc*-His bearing truncated *nqr*F without 1-72 nucleotides; $Ap^R$ | this work |
| pBAD_C377A | pBAD_NqrF′11; C377A substitution in NqrF′; $Ap^R$ | this work |
| pKnFhisAKm | pKNOCK bearing unidirectionally transcribed *nqr*F fused with $(His)_6$-tag, Km-resistance cassette, and *Apb*E; $Km^R$, $Tc^R$ | [22] |
| **Primers** | **Sequence*** | |
| NQRF'_dir | 5'-CTTTTCGCcAtGgCTAAGCTT | |
| pBAD_rev | 5'-TCATCCGCCAAAACAGC | |
| NQRFC377A_dir | 5'-GACTGTGAATACTACATGgcgGGcCCACCTATGATGAACG | |

* Nucleotides substituted during mutagenesis are designated by lower case letters and artificially introduced restriction sites are underlined.

cells were grown in this medium for 3 h. The cells were harvested by centrifugation (10,000*g*, 10 min) and washed twice with medium containing 300 mM NaCl, 10 mM Tris-HCl, and 5 mM $MgSO_4$ (pH 8.0). The cell pellet was suspended in medium containing 300 mM NaCl, 20 mM Tris-HCl, 5 mM $MgSO_4$, and 5 mM imidazole (pH 8.0), and the suspension was passed twice through a French press (16,000 psi). Cell debris and membrane vesicles were removed by centrifugation at 180,000*g* (60 min). The His-tagged NqrF′ was purified from the supernatant as described previously [22] but without addition of detergents to any of the column buffers.

**His-tagged $Na^+$-NQR complex** was purified from VHtag60 cells as described previously [22].

**NADH and dNADH oxidation by membrane vesicles and by purified $Na^+$-NQR** was measured using a Hitachi 557 spectrophotometer at 340 nm, 30°C. For membrane vesicles the measurements were performed in a medium containing 20 mM Tris-HCl (pH 8.0), 5 mM $MgSO_4$, and 100 mM KCl or NaCl. In the case of purified $Na^+$-NQR the reaction medium was supplemented with 0.025% DDM. To measure dNADH:$K_3$ oxidoreductase activity, menadione (50 μM) was also added to the reaction medium. The extinction coefficient $\varepsilon_{340}$ taken for NADH and dNADH was 6.22 $mM^{-1}\cdot cm^{-1}$. The apparent $K_m^{dNADH}$ values for dNADH oxidase activity in membrane vesicles were determined as described previously [24].

**3-D structure prediction for the fragment of the NqrF subunit of $Na^+$-NQR from *V. harveyi*.** The structure was predicted for the fragment of the NqrF subunit sequence starting from Ile126 and ending on Gly406. This part of the protein contains FAD- and NADH-binding motifs. For homology modeling the 128-412 a.a. domain of subunit F of $Na^+$-NQR from *P. gingivalis* with known crystal structure (PDB entry 2R6H, chain A) was used as a template. Selected sequence fragments sharing 53.1% of identity were aligned using ClustalX software. This alignment was submitted to the Swiss-Model server (http://swissmodel.expasy.org) [25] using an Alignment Mode for structure modeling of the NqrF fragment. The obtained 3-D model was refined by superposition of its coordinates with those of the template using the DeepView/Swiss-PdbViewer program [26]. To analyze the architecture of the electron input site, the docking of

FAD into the obtained model of *V. harveyi* NqrF fragment was performed. For this the resolved structure of the NqrF of $Na^+$-NQR from *P. gingivalis* containing FAD cofactor was superimposed with the modeled NqrF of $Na^+$-NQR from *V. harveyi* using VMD software. Then the coordinates of FAD resolved within the F subunit of *P. gingivalis* $Na^+$-NQR were translated into the modeled *V. harveyi* NqrF structure using the DeepView/Swiss-PdbViewer program.

***Thermo*FAD experimental setup.** Experiments were performed as described in [27] using an iCycler iQ real-time PCR detection system (Bio-Rad Laboratories, USA) with FAM-490 detection protocol. Unfolding curves (thermograms) were determined using a temperature gradient from 25 to 80°C, performing a fluorescence measurement within 10 sec after every 0.5°C increase step. The experiments were carried out in RT-PCR wells with medium containing 25 µl of 100 mM NaCl, 10 mM Hepes-Tris (pH 8.0), 0.1 mM EDTA, and ~15 µM of $Na^+$-NQR or NqrF′. In the case of $Na^+$-NQR the experimental medium was additionally supplemented with 0.05% DDM.

**FAD and riboflavin release from $Na^+$-NQR upon its thermodenaturation.** $Na^+$-NQR was unfolded using the temperature gradient from 25 to 80°C essentially as described above. At a desired temperature a sample was collected, cooled in ice, and the mixture of the protein and released soluble cofactors was immediately separated using a Microcon YM-10 centrifugal filter (Millipore, USA). The flavins from the obtained protein-free solution were analyzed by HPLC as described in [21].

**SDS-polyacrylamide gel electrophoresis** and detection of covalently bound flavins in $Na^+$-NQR were performed according to [2].

**Protein concentration** was determined using the bicinchoninic acid method with bovine serum albumin as a standard.

**$Na^+$-NQR concentration** was calculated using the known extinction coefficients: for oxidized $Na^+$-NQR, $\varepsilon_{465\text{-}520} = 43.4\ mM^{-1}\cdot cm^{-1}$; for the reduced *minus* oxidized $Na^+$-NQR spectrum, $\varepsilon_{465\text{-}770} = 44.3\ mM^{-1}\cdot cm^{-1}$ and $\varepsilon_{465\text{-}520} = 31.8\ mM^{-1}\cdot cm^{-1}$ [28].

## RESULTS AND DISCUSSION

**Structural analysis of the NqrF subunit of $Na^+$-translocating NADH:quinone oxidoreductase.** As mentioned above, $Ag^+$ is a specific inhibitor of the NADH-dehydrogenase and quinone reductase activities of $Na^+$-NQRs from different *Vibrio* species [17, 29]. This inhibition is apparently caused by modification of some cysteine residue in the NqrF subunit [7, 12, 19]. Recently, the structure of the NADH- and FAD-binding regions of NqrF from *Porphyromonas gingivalis* (PDB ID: 2R6H) and *V. cholerae* [30] has been determined by X-ray diffraction. Structure analysis of NqrF from *P. gingivalis* reveals that Cys383 is the main candidate for modification by $Ag^+$. As shown in Fig. 1a, this residue is located in close proximity (6.5 Å) to the noncovalently bound FAD. This means that the modification of Cys383 by heavy metal ions or by SH-reagents can prevent hydride ion transport from NADH to FAD and hence interrupt the $Na^+$-NQR activities. Even though Cys383 is partially shielded from the solvent by Phe411 and several other neighboring residues (see Fig. 1b), it can be accessible at least for small molecules.

All other cysteine residues in the FAD-binding domain of the NqrF subunit are distant from the NADH-dehydrogenase site and are embedded into the protein globule, i.e. they should be inaccessible to the solvent. This makes Cys383 with its reactive SH-group the only possible candidate for interaction with heavy metal ions and with SH-reagents.

Sequence alignment of NqrF subunits from various bacteria and of some of their homologous proteins (see Fig. 2) shows that $Cys_{NqrF}$-383 from *P. gingivalis* is absolutely invariant. It is present not only in all NqrF subunits but also in various ferredoxin:$NADP^+$ oxidoreductases. This allows testing the role of this residue in $Na^+$-NQR sensitivity to heavy metal ions by site-directed mutagenesis on the well-studied bacterium *V. harveyi*. Structure prediction of the NqrF subunit of $Na^+$-NQR from this bacterium showed that its Cys377, a counterpart of $Cys_{NqrF}$-383 from *P. gingivalis*, is also located at the atomic distance of 6.5 Å from the noncovalently bound FAD and is partially accessible for the solvent.

**Site-directed mutagenesis of Cys377 in the NqrF subunit of $Na^+$-NQR from *V. harveyi* and study of the mutant enzyme on membrane vesicles.** To test the involvement of $Cys_{NqrF}$-377 of $Na^+$-NQR from *V. harveyi* in interaction with silver ions, this residue was replaced by alanine using site directed mutagenesis, and the mutation was transferred into a *V. harveyi* chromosome. The strain obtained (FCA9) allowed us to study properties of the mutated $Na^+$-NQR in membrane vesicles as well as to purify this enzyme using affinity chromatography.

The ratio of NADH-dehydrogenase to quinone reductase activities of a $Na^+$-NQR preparation is a very useful indicator of its functional properties [31]. The respiratory chain of marine bacteria of genus *Vibrio* contains two different NADH:quinone oxidoreductases: $Na^+$-NQR and NDH-2 [12, 32]. It is known that various $Na^+$-translocating NADH:quinone oxidoreductases are able to oxidize either NADH or its analog dNADH, while noncoupled NADH:quinone oxidoreductases (NDH-2) oxidize only NADH, but not dNADH [12, 23]. Thus, it is possible to use dNADH oxidase and dNADH:$K_3$ oxidoreductase activities of membrane vesicles from *Vibrio* to determine the quinone reductase and NADH dehydrogenase activities of $Na^+$-NQR, respectively [12]. As shown earlier in [31], the ratio of

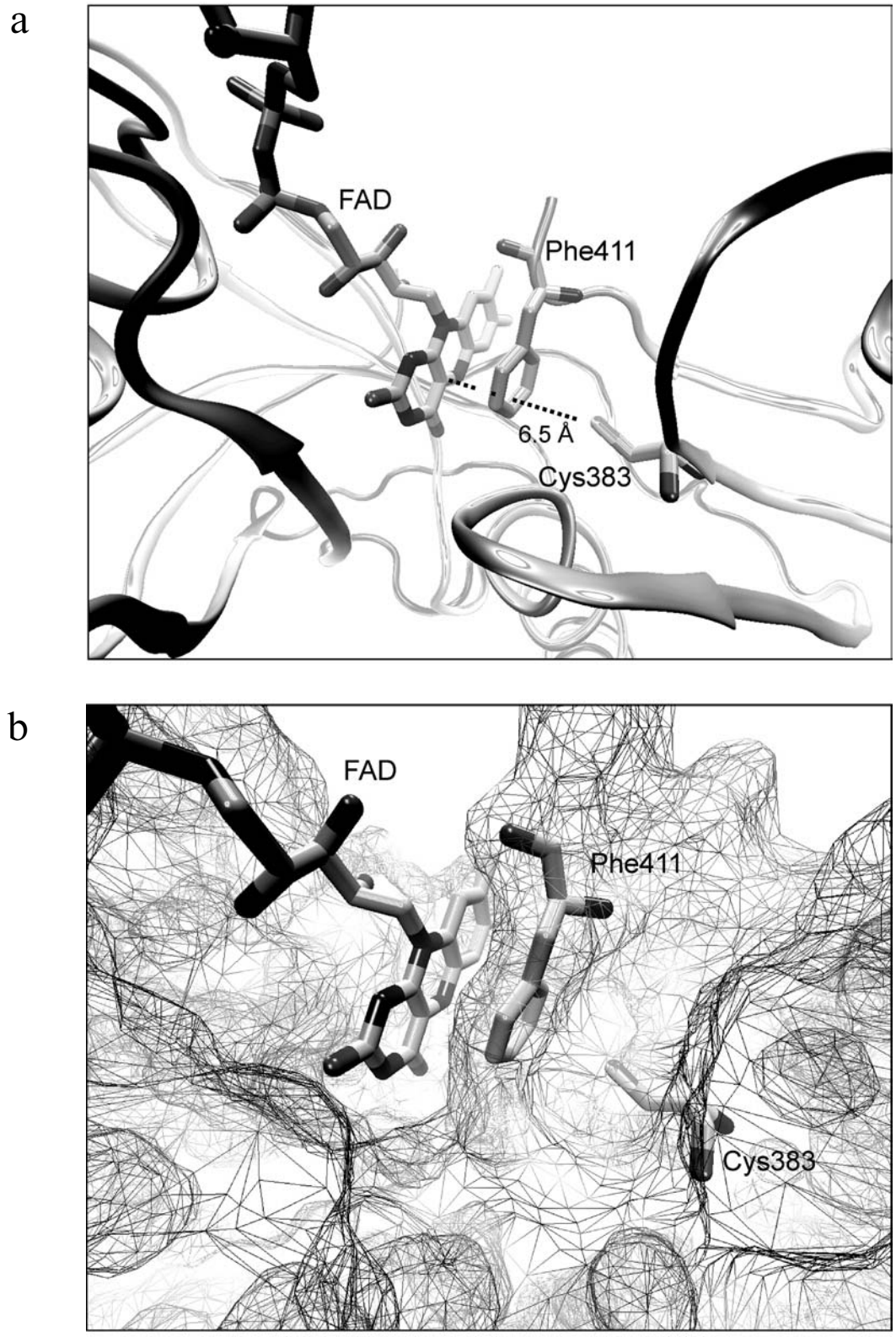


**Fig. 1.** a) Location of conserved Cys383 with respect to bound FAD in the NqrF subunit of $Na^+$-NQR from *P. gingivalis* (PDB entry 2R6H, chain A). The atomic distance between N(5) of the isoalloxazine ring of the FAD and the sulfur atom of the cysteine residue is shown in Å. b) The fragment of the molecular surface in the catalytic site of the NqrF subunit of $Na^+$-NQR from *P. gingivalis*. Positions of FAD and Cys383 spatially separated by Phe411 are shown. The picture was prepared using VMD software [38].


**Fig. 2.** Sequence alignment of C-terminal region of NqrF subunits and ferredoxin:$NADP^+$ oxidoreductases (FNR). NqrF_*Pgi*, NqrF from *P. gingivalis* (accession number NP_906227); NqrF_*Vha*, NqrF from *V. harveyi* (Q9RFV6); NqrF_*Kpn*, NqrF from *K. pneumoniae* (BAH61888); NqrF_*Nme*, NqrF from *Neisseria meningitidis* (YP_974604); NqrF_*Pae*, NqrF from *Pseudomonas aeruginosa* (NP_251684); FNR_*Ppu*, toluate 1,2-dioxygenase electron transfer component from *Pseudomonas putida* (NP_542869); FNR1_*Ath*, ferredoxin:$NADP^+$-oxidoreductase 1 from *Arabidopsis thaliana* (NP_201420). The conserved cysteine residue is marked by an asterisk.

dNADH:$K_3$ oxidoreductase to dNADH oxidase activities in membrane vesicles from a wild type *V. harveyi* strain is 1.8-1.9, see also Table 2. For membrane vesicles from the mutant strain FCA9 a similar ratio was determined (Table 2). However, the values of the specific dNADH:$K_3$ oxidoreductase and dNADH oxidase activities in the mutant strain were lower compared to the wild type cells. The dNADH oxidase activity of membrane vesicles from the mutant strain FCA9 was stimulated by sodium ions similarly to the wild type strain, and this activity was sensitive to the specific $Na^+$-NQR inhibitor HQNO to the same extent as in the control strain VHtag60 (Table 2). Thus, replacement of $Cys_{NqrF}$-377 by alanine in $Na^+$-NQR from *V. harveyi* decreases the specific activities of the enzyme in membrane vesicles but is not accompanied by significant changes in its other main functional properties.

**Sensitivity of the mutant variant of $Na^+$-NQR to heavy metal ions.** As shown earlier in [12] and as seen in Fig. 3, addition of 1 μM $Ag^+$ to the reaction medium leads to almost complete inhibition of the dNADH oxidase activity of membrane vesicles isolated from a wild type strain of *V. harveyi*. After replacement of the $Cys_{NqrF}$-377 with Ala, this activity became resistant to micromolar concentrations of silver ions (Fig. 3).

It was demonstrated earlier that the $Na^+$-NQR activities are also inhibited by other heavy metal ions ($Cd^{2+}$, $Pb^{2+}$, $Zn^{2+}$, and $Cu^{2+}$) [13]. We addressed the question of whether these ions inhibit the enzyme similarly to silver ions by modification of $Cys_{NqrF}$-377. As shown in Table 3, addition of 100 μM of $Cd^{2+}$, $Zn^{2+}$, or $Cu^{2+}$ to the reaction medium resulted in almost complete inhibition of dNADH:$K_3$ oxidoreductase activity of membrane vesicles from the wild type strain. In contrast, in the case of the mutant strain the same addition of $Cd^{2+}$ or $Zn^{2+}$ had no effect on the activity, and addition of $Cu^{2+}$ resulted only in its minor decrease. The same results were obtained when NEM, a SH-reagent, was used as an inhibitor (data not shown). These results indicate that the $Na^+$-NQR inactivation by $Ag^+$ as well as by other heavy metal ions is caused by modification of the conserved Cys377 in the NqrF subunit.

It is known that $Na^+$-NQRs from different bacterial sources have different sensitivity to $Ag^+$ and NEM [12]. For example, in spite of the presence of the conserved cysteine residue (corresponding to $Cys_{NqrF}$-377 in *V. harveyi*) in $Na^+$-NQR from *K. pneumoniae* (see Fig. 2), this enzyme is shown to be fully resistant to both $Ag^+$ and NEM [12]. Moreover, it is known that ferredoxin:$NADP^+$ oxidoreductases, which also contain this cysteine residue (see Fig. 2), are insensitive to submillimolar concentrations of heavy metals as well [33]. Therefore, the different sensitivity of $Na^+$-NQRs from diverse bacterial sources is determined rather by different *accessibility* of the con-

**Table 2.** Rates of NADH and dNADH oxidation by membrane vesicles isolated from different *V. harveyi* strains

| Strain | Activity[a] | | | Ratio[b] |
|---|---|---|---|---|
| | dNADH oxidase | dNADH:$K_3$ oxidoreductase | NADH oxidase | |
| *V. harveyi* VHtag60 (wild type) | 0.20 (+)*(+)** | 0.37 | 0.35 | 1.8 |
| *V. harveyi* FCA9 ($_{NqrF}$C377A) | 0.06 (+)*(+)** | 0.11 | 0.46 | 1.8 |

* Stimulation of activity by sodium ions.
** Sensitivity of activity to HQNO (4 μM).
[a] Activities are given in μmol of (d)NADH oxidized per min per mg protein, data of a typical experiment are shown.
[b] Ratio of dNADH:$K_3$ oxidoreductase to dNADH oxidase activities.

served cysteine residue ($Cys_{NqrF}$-377 in *V. harveyi*) than by different *content* of this amino acid.

Thus, the site-directed mutagenesis of $Cys_{NqrF}$-377 brings rather surprising results. On one hand, as expected the replacement of this residue results in resistance of $Na^+$-NQR to heavy metal ions. On the other hand, in spite of absolute invariance of this cysteine residue in the primary sequences of NqrFs and of the other homologous proteins, its replacement is not accompanied by significant changes in the main functional properties of the enzyme other than sensitivity to heavy metals. However, it is difficult to imagine that Cys377 was evolutionally conserved just to make $Na^+$-NQR activity sensitive to SH-modifying reagents. In other words, the Cys377 replacement should be presumably connected with some other changes in the characteristics of $Na^+$-NQR. This prompted us to study properties of $Na^+$-NQR with $_{NqrF}$C377A replacement in more detail.

Only one distinction of the mutant variant of the enzyme has been detected. As mentioned above, the specific $Na^+$-NQR activities in membrane vesicles from the mutant FCA9 strain were lower compared to the wild type strain (see Table 2). This effect can be hypothetically linked with decrease in the enzyme affinity to dNADH. However, determination of the apparent $K_m^{dNADH}$ on the membrane vesicles from the mutant and control strains using the dNADH-oxidase activity showed that $_{NqrF}$C377A replacement even caused increase in the apparent $Na^+$-NQR affinity to dNADH and resulted in about 3-times lower $K_m$ than in the wild type; $K_m = 14.7 \pm 0.3$ μM *versus* $K_m = 46.5 \pm 1.2$ μM for the mutant and wild type strains, respectively. Thus the low specific activities of the mutant $Na^+$-NQR in the membrane vesicles could be caused by either decrease in the catalytic constant value ($k_{cat}$) or decrease in the protein stability, which leads to lower content of the active enzyme in the membranes. To distinguish between these alternatives, we compared the activity and stability of the purified mutant and wild type enzymes.

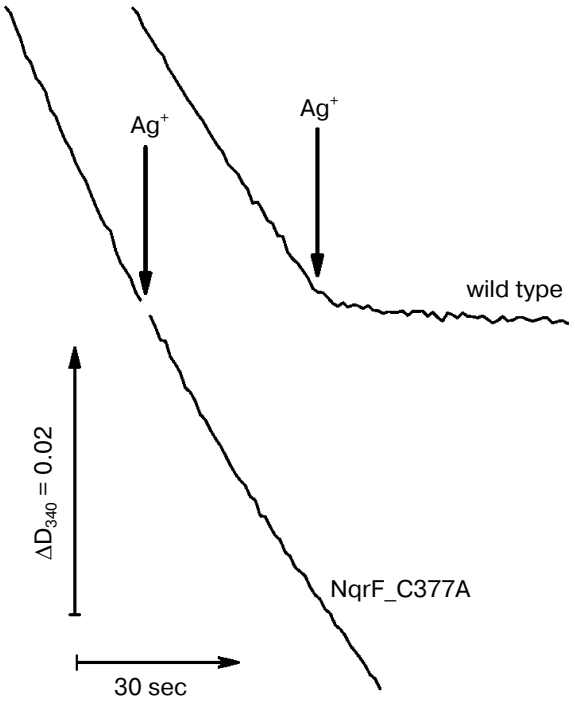


**Fig. 3.** Inhibition of dNADH oxidase activity by $Ag^+$ measured in membrane vesicles isolated from *V. harveyi* VHtag60 (wild type) or from *V. harveyi* FCA9 ($_{NqrF}$C377A) strains. Activities were measured in medium containing 20 mM Tris-HCl (pH 8.0), 5 mM $MgSO_4$, 100 mM NaCl. Additions: $AgNO_3$, 1 μM.

**Table 3.** Inhibition of dNADH:$K_3$ oxidoreductase activity of membrane vesicles from VHtag60 (wild type) and FCA9 ($_{NqrF}$C377A) *V. harveyi* strains by heavy metal ions

| Heavy metal | Residual activity, % | |
|---|---|---|
| | wild type | $_{NqrF}$C377A |
| $Zn^{2+}$ (100 μM) | 7 | 94 |
| $Cd^{2+}$ (100 μM) | 2 | 100 |
| $Cu^{2+}$ (100 μM) | 11 | 68 |

**Characterization of catalytic properties of purified $Na^+$-NQR with $_{NqrF}$C377A replacement.** The wild type and the $_{NqrF}$C377A variants of $Na^+$-NQR were purified from the corresponding *V. harveyi* cells using affinity chromatography, and the main properties of these proteins were determined. Analysis by SDS-PAGE showed that the purified $_{NqrF}$C377A $Na^+$-NQR had the same subunit composition as the wild type enzyme. Measurement of the fluorescence intensity of covalently bound flavins in the purified enzymes revealed that the amount of these prosthetic groups is equimolar to protein content in both wild type and mutant $Na^+$-NQR proteins. The optical spectrum of the mutant enzyme was similar to that of the wild type $Na^+$-NQR (data not shown).

The known extinction coefficients for the purified $Na^+$-NQR [28] allow determination of the specific enzyme activity in turnovers per second, i.e. to compare the real $k_{cat}$ values for different enzyme preparations. It was shown that the replacement of the $Cys_{NqrF}$-377 results in about 14-fold decrease in $Na^+$-NQR enzymatic activity. In the case of the NADH-dehydrogenase reaction, the activity values were $51 \pm 9$ and $740 \pm 50$ $sec^{-1}$ for the mutant and the wild type enzymes, respectively. It is noteworthy that the same results were earlier obtained for spinach FNR. The C272S mutant (the counterpart of the $Cys_{NqrF}$-377 from *V. harveyi*) FNR showed a 35-fold reduction in catalytic efficiency with respect to the wild type enzyme due to a substantial decrease in $k_{cat}$ [34].

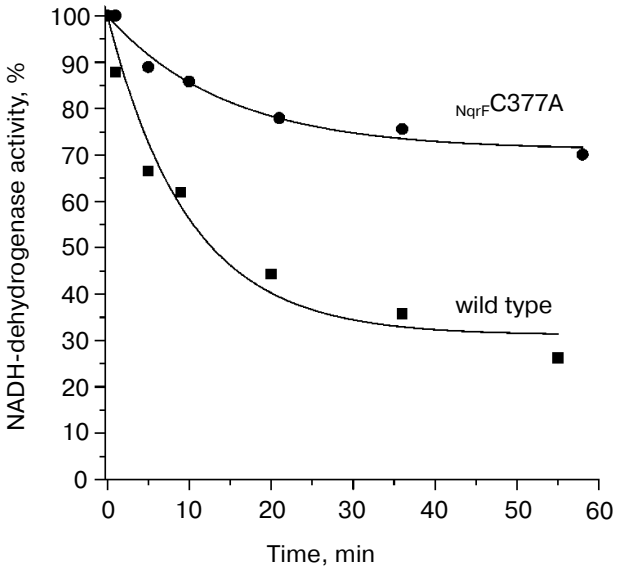


**Fig. 4.** Inhibition of NADH-dehydrogenase activity of purified wild type (squares) and the $_{NqrF}$C377A mutant (circles) $Na^+$-NQR upon aerobic incubation of the enzymes with NADH. Data of a typical experiment are shown. The wild type (0.3 mg protein per ml) and the mutant $_{NqrF}$C377A (0.9 mg/ml) $Na^+$-NQRs were incubated at 30°C in medium containing 10 mM Tris-HCl (pH 8.0), 200 mM NaCl, and 0.05% DDM. The mixture was supplemented with NADH (5 mM), and the rates of NADH-dehydrogenase activity were measured at appropriate time points.

Purified preparations of the enzyme allowed us to test the involvement of $Cys_{NqrF}$-377 in some additional properties of $Na^+$-NQR. It is known that this enzyme in purified form undergoes irreversible inactivation during aerobic incubation with NADH in the absence of electron acceptors [35]. As shown in Fig. 4, the inactivation of the $_{NqrF}$C377A $Na^+$-NQR variant proceeded significantly slower compared to the wild type enzyme. Thus, it seems that $Na^+$-NQR inactivation under aerobic incubation with NADH is caused, at least partially, by oxidation of $Cys_{NqrF}$-377.

**Thermostability of purified $Na^+$-NQR complexes as well as isolated NqrF′ (soluble variant of NqrF) subunits.** To compare the stability of mutated and wild type $Na^+$-NQR complexes, the so-called "*Thermo*FAD" method [27] was used. In this technique, the flavin cofactor is exploited as an intrinsic probe to monitor protein folding and stability, taking advantage of the different fluorescent properties of flavin-containing proteins between the folded and denatured state. As the fluorescence of flavin cofactors in flavoproteins is usually quenched by the protein environment when the protein is properly folded [36], it is possible to measure the unfolding temperature of a flavoprotein by monitoring the increase in the fluorescence of the cofactor [27].

A typical thermogram for the wild type $Na^+$-NQR complex is shown in Fig. 5a. As can be seen, it consists of two overlapping sigmoidal curves: one with a sharp slope having unfolding temperature value $T_m$ = 50°C, and the other with a gentle slope and $T_m \approx 62$°C (the unfolding temperatures were determined as the maxima of the derivative of the direct curve, see Fig. 5b). Since $Na^+$-NQR contains four different flavins as prosthetic groups [9, 37], the thermogram (Fig. 5) should be the sum of the unfolding processes taking place in four different flavin-binding domains of the enzyme. To attribute the unfolding of the FAD-binding domain from the NqrF subunit to

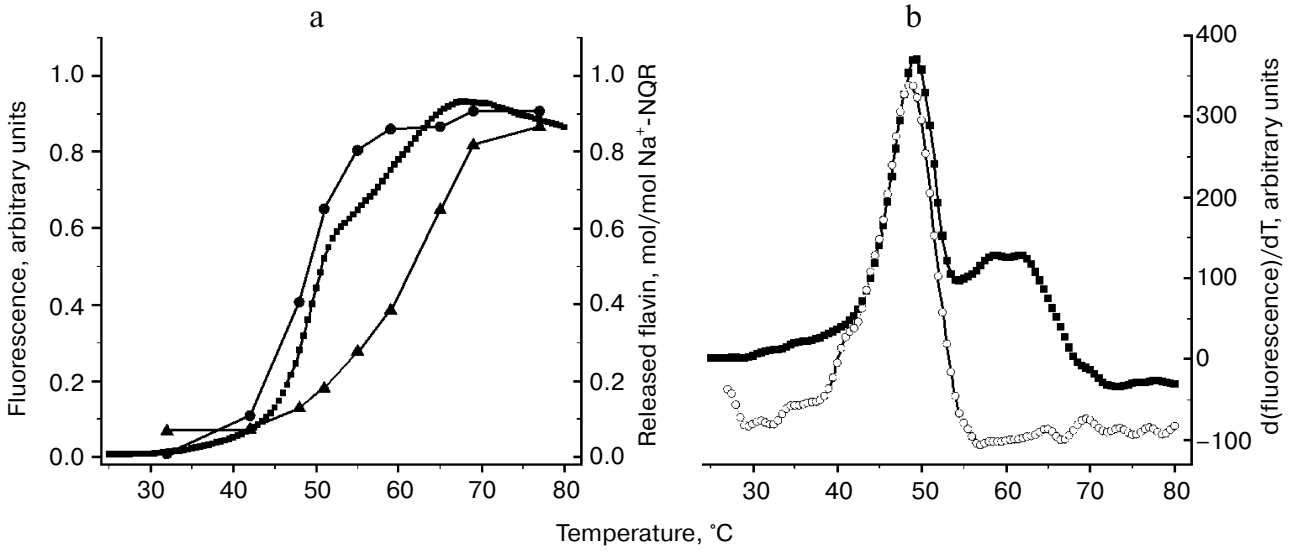


**Fig. 5.** a) Thermal stability of the wild type $Na^+$-NQR complex determined by changes in flavin fluorescence (squares, the left ordinate axis), or by measurement of FAD (circles) and riboflavin (triangles) release (the right ordinate axis). b) Thermal stability curves of the wild type $Na^+$-NQR complex (closed squares) in comparison with the isolated wild type NqrF subunit (open circles) determined by changes in flavin fluorescence.

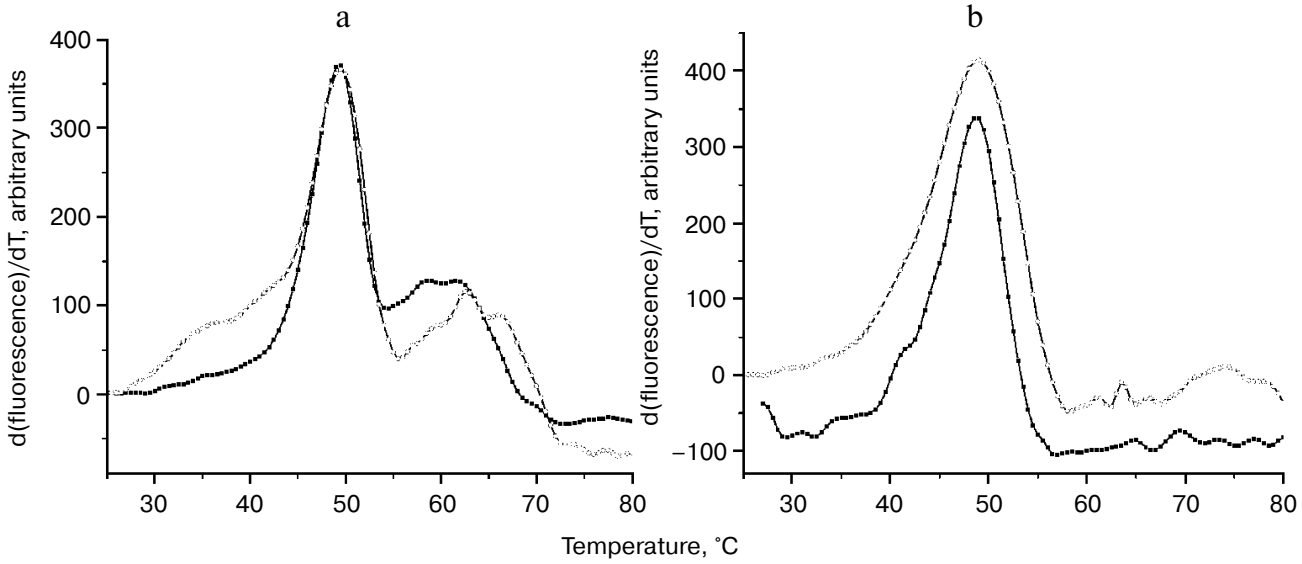


**Fig. 6.** a) Thermal stability of wild type (closed squares) and $_{NqrF}$C377A (open circles) $Na^+$-NQR complexes. b) Thermal stability curves for the wild type (closed squares) and $_{NqrF}$C377A (open circles) NqrF′ subunits. Unfolding processes were determined by measurement of changes in flavin fluorescence.

one of the determined transitions, we measured a thermogram for the isolated wild type NqrF′ subunit (Fig. 5b). Melting of this subunit matched the low-temperature transition in the entire $Na^+$-NQR complex not only by the $T_m$ value, but also by the shape of the curve. The kinetics of release of different flavins from $Na^+$-NQR during the time course of thermodenaturation has also been studied. As can bee seen in Fig. 5a, the release of FAD corresponds to the low-temperature transition in $Na^+$-NQR with $T_m$ = 50°C, while riboflavin release is related to the high-temperature transition with $T_m$ = 62°C. These results indicate that the transition with $T_m$ = 50°C corresponds to unfolding of the FAD-binding domain of the NqrF, while the transition with $T_m$ = 62°C is melting of the riboflavin-binding domain from the yet unrecognized subunit. Unfortunately, because two FMN residues are covalently bound to $Na^+$-NQR, it was impossible to establish the unfolding temperatures for FMN-binding domains of the NqrB and NqrC subunits.

The "*Thermo*FAD" technique was also used to compare stability of the $_{NqrF}$C377A variants of either isolated NqrF′ subunit or $Na^+$-NQR complex with corresponding proteins of the wild type. As can be seen in Fig. 6 (a and b), the thermograms of these proteins are very similar. The $_{NqrF}$C377A mutation resulted in a slight broadening of the peak corresponding to the unfolding of the FAD-binding domain without any shift of its $T_m$. These data indicate that Cys377 replacement in NqrF subunit does not lead to destabilization of $Na^+$-NQR. These data are in agreement with the results of thermoinactivation of the enzymatic activity of $Na^+$-NQR. At 48°C the wild type and the $_{NqrF}$C377A variants of $Na^+$-NQR complex were inactivated with about the same rates ($k_{obs}$ = 0.085 $sec^{-1}$ and $k_{obs}$ = 0.093 $sec^{-1}$, respectively).

While antibacterial effects of silver salts were first noticed long ago, $Na^+$-NQR has been recently recognized as one of the targets for $Ag^+$ [17, 29]. Since $Na^+$-NQR is widespread among pathogenic microorganisms [2, 3], silver containing compounds were even proposed to be an attractive potential target for the development of "smart" drugs and therapeutic strategies that would have minimal side effects at acceptable antimicrobial potency [3]. In the present work on $Na^+$-NQR from *V. harveyi*, it was demonstrated that inhibition of the enzyme by $Ag^+$ and by other heavy metal ions is mediated by modification of its conserved $Cys_{NqrF}$-377 residue. It was also shown that the $Cys_{NqrF}$-377 mutation affects only the rate of NADH oxidation, making the input of electrons into the enzyme of about 14-times slower than in the wild type $Na^+$-NQR, whereas all other properties of the enzyme including the stability remain unchanged.

We thank Dr. C. C. Hase for providing us with the *V. cholerae* strain.

This work was supported by the Russian Foundation for Basic Research (project number 10-04-00352).

## REFERENCES

1. Bogachev, A. V., and Verkhovsky, M. I. (2005) *Biochemistry (Moscow)*, **70**, 143-149.
2. Zhou, W., Bertsova, Y. V., Feng, B., Tsatsos, P., Verkhovskaya, M. L., Gennis, R. B., Bogachev, A. V., and Barquera, B. (1999) *Biochemistry*, **38**, 16246-16252.

3. Hase, C. C., Fedorova, N. D., Galperin, M. Y., and Dibrov, P. A. (2001) *Microbiol. Mol. Biol. Rev.*, **65**, 353-370.
4. Nakayama, Y., Hayashi, M., and Unemoto, T. (1998) *FEBS Lett.*, **422**, 240-242.
5. Rich, P. R., Meinier, B., and Ward, B. (1995) *FEBS Lett.*, **375**, 5-10.
6. Hayashi, M., Hirai, K., and Unemoto, T. (1995) *FEBS Lett.*, **363**, 75-77.
7. Turk, K., Puhar, A., Neese, F., Bill, E., Fritz, G., and Steuber, J. (2004) *J. Biol. Chem.*, **279**, 21349-21355.
8. Barquera, B., Nilges, M. J., Morgan, J. E., Ramirez-Silva, L., Zhou, W., and Gennis, R. B. (2004) *Biochemistry*, **43**, 12322-12330.
9. Juarez, O., Nilges, M. J., Gillespie, P., Cotton, J., and Barquera, B. (2008) *J. Biol. Chem.*, **283**, 33162-33167.
10. Hayashi, M., Nakayama, Y., Yasui, M., Maeda, M., Furuishi, K., and Unemoto, T. (2001) *FEBS Lett.*, **488**, 5-8.
11. Bogachev, A. V., Murtasina, R. A., and Skulachev, V. P. (1997) *FEBS Lett.*, **409**, 475-477.
12. Fadeeva, M. S., Nunez, C., Bertsova, Y. V., Espin, G., and Bogachev, A. V. (2008) *FEMS Microbiol. Lett.*, **279**, 116-123.
13. Bourne, R. M., and Rich, P. R. (1992) *Biochem. Soc. Trans.*, **20**, 577-582.
14. Hayashi, M., and Unemoto, T. (1984) *Biochim. Biophys. Acta*, **767**, 470-478.
15. Yoshikawa, K., Nakayama, Y., Hayashi, M., Unemoto, T., and Mochida, K. (1999) *J. Antibiot.*, **52**, 182-185.
16. Tokuda, H., and Unemoto, T. (1984) *J. Biol. Chem.*, **259**, 7785-7790.
17. Asano, M., Hayashi, M., Unemoto, T., and Tokuda, H. (1985) *Agric. Biol. Chem.*, **49**, 2813-2817.
18. Hayashi, M., Shibata, N., Nakayama, Y., Yoshikawa, K., and Unemoto, T. (2002) *Arch. Biochem. Biophys.*, **401**, 173-177.
19. Unemoto, T., Ogura, T., and Hayashi, M. (1993) *Biochim. Biophys. Acta*, **1183**, 201-205.
20. Fadeeva, M. S., Yakovtseva, E. A., Belevich, G. A., Bertsova, Y. V., and Bogachev, A. V. (2007) *Arch. Microbiol.*, **188**, 341-348.
21. Bogachev, A. V., Bertsova, Y. V., Bloch, D. A., and Verkhovsky, M. I. (2006) *Biochemistry*, **45**, 3421-3428.
22. Bogachev, A. V., Kulik, L. V., Bloch, D. A., Bertsova, Y. V., Fadeeva, M. S., and Verkhovsky, M. I. (2009) *Biochemistry*, **48**, 6291-6298.
23. Bertsova, Y. V., and Bogachev, A. V. (2004) *FEBS Lett.*, **563**, 207-212.
24. Bogachev, A. V., Belevich, N. P., Bertsova, Y. V., and Verkhovsky, M. I. (2009) *J. Biol. Chem.*, **284**, 5533-5538.
25. Schwede, T., Kopp, J., Guex, N., and Peitsch, M. C. (2003) *Nucleic Acids Res.*, **31**, 3381-3385.
26. Guex, N., and Peitsch, M. C. (1997) *Electrophoresis*, **18**, 2714-2723.
27. Forneris, F., Orru, R., Bonivento, D., Chiarelli, L. R., and Mattevi, A. (2009) *FEBS J.*, **276**, 2833-2840.
28. Bogachev, A. V., Bloch, D. A., Bertsova, Y. V., and Verkhovsky, M. I. (2009) *Biochemistry*, **48**, 6299-6304.
29. Steuber, J., Krebs, W., and Dimroth, P. (1997) *Eur. J. Biochem.*, **249**, 770-776.
30. Tao, M., Casutt, M., Diez, J., Fritz, G., and Steuber, J. (2008) *Biochim. Biophys. Acta*, **1777**, S39.
31. Fadeeva, M. S., Bertsova, Y. V., Verkhovsky, M. I., and Bogachev, A. V. (2008) *Biochemistry (Moscow)*, **73**, 123-129.
32. Hayashi, M., Miyoshi, T., Sato, M., and Unemoto, T. (1992) *Biochim. Biophys. Acta*, **1099**, 145-151.
33. Grzyb, J., Waloszek, A., Latowski, D., and Wieckowski, S. (2004) *J. Inorg. Biochem.*, **98**, 1338-1346.
34. Aliverti, A., Piubelli, L., Zanetti, G., Lubberstedt, T., Herrmann, R. G., and Curti, B. (1993) *Biochemistry*, **32**, 6374-6380.
35. Pfenninger-Li, X. D., Albracht, S. P. J., van Belzen, R., and Dimroth, P. (1996) *Biochemistry*, **35**, 6233-6242.
36. Munro, A. W., and Noble, M. A. (1999) *Meth. Mol. Biol.*, **131**, 25-48.
37. Verkhovsky, M. I., and Bogachev, A. V. (2010) *Biochim. Biophys. Acta*, **1797**, 738-746.
38. Humphrey, W., Dalke, A., and Schulten, K. (1996) *J. Mol. Graph.*, **14**, 33-38.
39. Barquera, B., Hellwig, P., Zhou, W., Morgan, J. E., Hase, C. C., Gosink, K. K., Nilges, M., Bruesehoff, P. J., Roth, A., Lancaster, C. R., and Gennis, R. B. (2002) *Biochemistry*, **41**, 3781-3789.
40. Miller, S., and Mekalanos, J. (1988) *J. Bacteriol.*, **170**, 2575-2583.